공학석사 학위논문

# 낮은 시멘트에서다량의 세노스피어의 혼입을 통한 고강도 및 경량 시멘트 복합체 개발

Incorporation of a high volume of cenosphere particles in low water-to-cement matrix for developing high strength & lightweight cementitious composites

2021 년 8 월

서울대학교 대학원

건설환경공학부

JYOTI MAHATO

**Incorporation of a high volume of cenosphere particles in low water-to-cement matrix for developing high strength & lightweight cementitious composites**

지도 교수 문주혁

이 논문을 공학석사 학위논문으로 제출함

2021 년 8 월

서울대학교 대학원

건설환경공학부

**JYOTI MAHATO**

JYOTI MAHATO 의 석사 학위논문을 인준함

2021 년 08 월

위 원 장 조재열

부위원장 문주혁

위 원 김호경

# Incorporation of a high volume of cenosphere particles in low water-to-cement matrix for developing high strength & lightweight cementitious composites

낮은 물-시멘트에서 다량의 세노스피어의 혼입을

통한 고강도 및 경량 시멘트 복합체 개발

By

Jyoti Mahato

Advisor: Juhyuk Moon

A dissertation submitted in partial fulfilment of the requirements for the degree of Master in Civil and Environmental Engineering

August, 2021

Department of Civil and Environmental Engineering

College of Engineering

Seoul National University

**Abstract**

# Incorporation of a high volume of cenosphere particles in low water-to-cement matrix for developing high strength & lightweight cementitious composites

**Jyoti Mahato**[1]

**Department of Civil and Environmental Engineering**

**College of Engineering**

**Seoul National University**


The rapid increase of infrastructure and urbanization demand for low-density concrete. Low-density concrete can be achieved by incorporating lightweight aggregates in concrete but at the same time compromises the strength. Additionally, lightweight concrete is susceptible to aggregate segregation due to the low density of the lightweight aggregates. Furthermore,


[1] The author of this thesis is a Global Korea Scholarship scholar sponsored by the Korean Government

global warming urges the use of energy-efficient and energy-saving concrete materials. Therefore, this study aims to develop lightweight cementitious composites with high compressive strength and low density and low thermal conductivity properties using a byproduct of flyash i.e. cenospheres

In this experimental program, cenospheres were added in the mixture to 10 and 20 wt% in low water to cement ratio. Also, two different temperatures: ambient temperature (20 ºC and RH 60%) and heat treatment (90 ºC) were used for curing the specimens. Compressive strength, thermal conductivity, and density of the mixtures were determined. Additionally, X-ray diffraction (XRD) and thermogravimetric analysis (TGA) were performed to obtain the mineralogical characteristics and qualitatively analyze phase transformations of the hydrated phases, respectively. Segregation of the cenospheres and the internal microstructure of the specimens were also studied using micro-computed tomography.

The results demonstrated that the developed composites had remarkable compressive strength as of 74~64 MPa cured at ambient temperature (20 ºC and RH 60%) and 90~87 MPa cured at heat treatment (90 ºC). Besides, it also exhibited low density and low thermal conductivity. Furthermore, the adopted mix design overcomes the problem of segregation phenomena i.e., uniform dispersion of cenospheres in the mix was confirmed via micro-computed

tomography and the quantification of this phenomenon was calculated. Moreover, the porosity results show that the developed composites have great potential to be used in structures that are exposed to saline environments.

**Keywords**: Lightweight composites; Cenosphere; Thermal conductivity; Micro-computed Tomography; Porosity

**Student number: 2019-27932**

# Table of contents

# List of tables

# List of figures

# Chapter 1. Introduction

## 1.1. General background

The use of lightweight concrete can reduce the mass of the structures, thereby decreasing the seismic responses and minimizing the risk of earthquake damage. Besides, lightweight concrete has other properties such as better thermal insulation for energy-efficient building structures and can also reduce the dimension of sections of structural elements [1]. Therefore, there is an increasing need to develop high strength and lightweight concrete, due to the dramatic growth of civil structures such as high-rise buildings, long-span bridges, very large floating structures [1, 2].

The concrete that has a compressive strength greater than 60 MPa and a dry density less than 1920 kg/m$^3$, is classified as high strength lightweight concrete [2]. Recently, diverse ways to produce and modify lightweight concrete have been investigated using lightweight aggregates such as hollow micro-glass, pumice [3, 4], expanded perlite [5, 6] in cementitious materials. Although using these materials as aggregates can reduce the density and thermal conductivity of concrete, they reduce the compressive strength too. Furthermore, the low density of these porous aggregates leads to the floatation of aggregates upward in the concrete. Consequently, this may cause heterogeneity in the mix, variations in porosity that can affect the mechanical and durable properties of the concrete.

### 1.2. Motivation

Cenospheres are lightweight fillers that can be used to overcome the aforementioned issues. Cenospheres are an industrial waste byproduct of coal power plants [7]. They are hollow particles whose size generally range from 10 to 400 μm [8]. The density of the cenospheres ranges from 400 to 900 kg/m$^3$ [9]. Although after the combustion of coal, flyash has been used as supplementary cementitious material, however, the amount being used is small and leaving a great portion of them disposed on the landfills or in the water bodies causing a serious environmental problem. In 2015, China itself produces over 600 million tons of coal flyash which is double that in 2005, which indicates that production is increasing at an alarming rate [10]. Moreover, it is estimated that approximately 750 million tons of flyash are produced worldwide annually. Thus, the use of cenospheres in lightweight concrete, chosen in this study can be sustainable material. Hence, using cenospheres in the cementitious materials of lightweight concrete can create an effective avenue to eliminate the problem of improper disposal which can result in minimizing its detrimental effects on the environment [11].

From the previous studies, the lowest water to cement ratio (0.3 to 0.26) along with the smaller size of cenospheres used so far in the mix was only reported in the study of Zhou and Brooks et al. 2019 [12]. Very few studies exhibiting compressive strength higher than 60 MPa have been developed yet

[13, 14]. A majority of the previous studies on lightweight concrete were mainly focused on achieving a low density of concrete. Furthermore, there is a very limited study on the concrete having high strength along with low density and low thermal conductivity. Additionally, the effect of different curing temperatures on the mix containing cenospheres has not been investigated till now. Also, the study of segregation phenomenon in lightweight concrete has been limited.

### 1.3. Objectives of this study

The purpose of the present study is to develop composites having high strength and low-density cementitious composites using cenospheres in a low water-cement ratio of 0.23. Different curing conditions with varying cenospheres content were investigated. The developed composites showed the highest compressive strength of 74 MPa at ambient curing and 90 MPa with heat treatment at 10% cenospheres content. It was worth mentioning that all the mix types fulfill the safer limit criteria for density and thermal conductivity of lightweight concrete. Furthermore, X-ray diffraction (XRD) and thermogravimetric analysis (TGA) were performed for examining the hydration reaction of the developed composites. The internal microstructure study of the hydrated specimens and segregation of cenospheres in the mix were examined using micro-computed tomography.

# Chapter 2. Literature Review

## 2.1. Different ways of production of lightweight concrete

Lightweight concrete has been known since ancient times, back in 3000 BC which was made using natural aggregates of volcanic origin such as pumice, scoria, etc. During the Roman and Greek Empire, some ancient structures were built using natural aggregates such as St. Sofia Cathedral in the 4$^{th}$ century A. D, Roman temple, Pantheon, which was built during 118 to 128 A. D [15]. Still some natural aggregates such as pumice, are still in use as an aggregate in countries such as Germany, Italy, Iceland, and Japan. Palm oil shells are also used for making lightweight aggregate concrete such as in Malaysia. In 1918, Stephen J. Hayde patented the lightweight aggregate named "Haydite" which was the first synthetic aggregates made by the expansion of shale in the United States [15].

There are three ways/types of the production of lightweight concrete. They are as follows

a. No fines concrete: Concrete composed of cement and coarse aggregate of 9 -19 mm are known as no fines concrete. It creates air-filled voids by removing fine aggregates. Hence, it has voids, which are uniformly distributed throughout the mass. This process was first done by Wimpey in 1942 and is mainly used for the structures such as

partition walls and other non-structural construction. This is due to an agglomeration of coarse aggregate particles which create large pores within the body of the concrete and are responsible for its low strength.

b. Autoclaved aerated concrete or foamed concrete (AAC): Aerated concrete is a lightweight, cellular material made of cement or lime, sand, and other siliceous material and does not contain coarse aggregates due to which it has the lowest density, thermal conductivity, and strength. It is made by inserting gas bubbles in a cement paste or mortar matrix forming 30-50% voids. Either by chemical reaction or by using air entraining agent, voids are introduced. High-pressure steam cured aerated concrete is generally used as the structural material. It is thus, manufactured as the precast units for floors, walls, and roofs.

c. Lightweight aggregate concrete (LWAC): In this type of LWAC, natural aggregates in a concrete mix are replaced partially or wholly with the lightweight aggregates containing voids such as clay expanded perlite, slate. Also, the production of the new types of an artificial lightweight aggregate made it possible to introduce high-strength lightweight concrete which is suitable for structural works. It is mainly used for precast blocks or steel reinforcements.

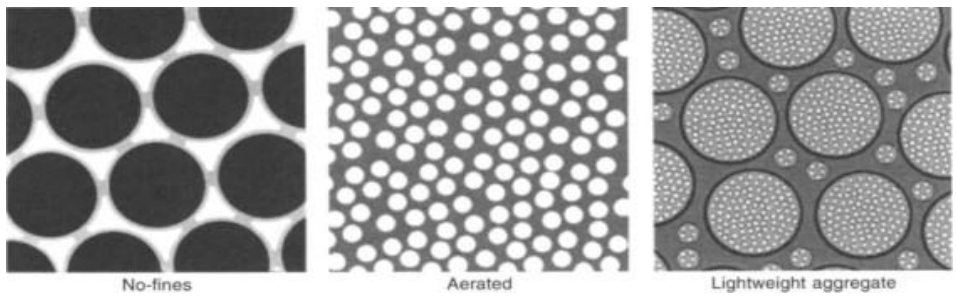


**Figure 1.** Basic forms of lightweight concrete [16]

There are two different lightweight aggregates types used as LWAC and are classified as below:

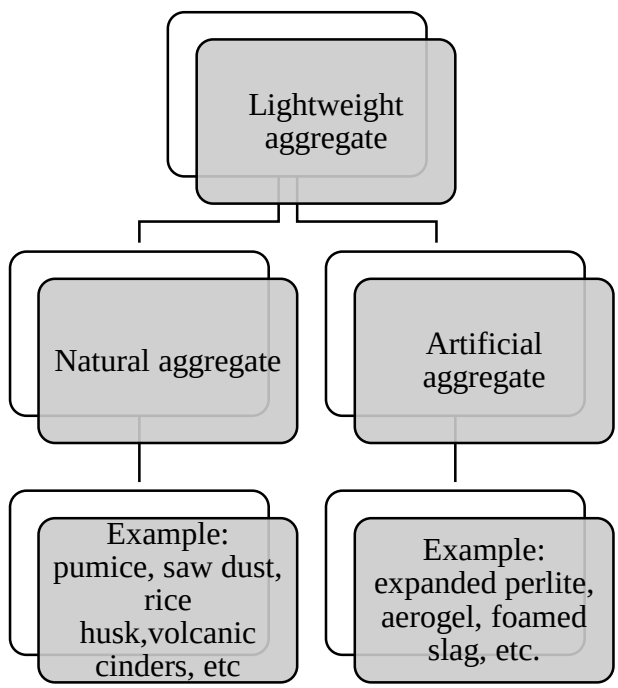


Based on the strength, lightweight concrete is divided into three categories according to ACI -213 guide for structural lightweight aggregate.

1. Low-density concrete: Compressive strength ranges in between (0.7-2) MPa with the density in the range of (300-800) kg/$m^3$.
2. Moderate strength concrete: Compressive strength ranges in between (7-14) MPa and density varies in between (800-1350) kg/$m^3$.
3. Structural concrete: Compressive strength and density range from 17 to 63 MPa and 1350-1920 kg/$m^3$, respectively.

### 2.2. Various types of lightweight aggregates used in the previous studies

Numerous studies have replaced natural aggregates partly or totally with artificial aggregates for lightweight concrete. Artificial aggregate such as aerogel, made of silica having nanoporous material, resulted in the lightweight and thermal insulating concrete with 8.3 Mpa compressive strength at 60% volume of aerogel [17]. Similarly, glass microspheres along with the polyethylene fibers were used for building floating concrete structures, insulating elements [18]. Furthermore, structural lightweight cementitious composites with a high insulation capacity and satisfactory compressive strength of 45 Mpa were developed using expanded polystyrene in the study of Dixit et al., 2019 [19]. In this study, a byproduct of flyash i.e. cenospheres as a lightweight filler was used to develop high strength and lightweight cementitious composites.

### 2.2.1. Cenospheres

Cenospheres are the hollow aluminate silicate particles obtained as a residue from coal-fired power plants. Cenospheres are the combination of two Greek words: ‘Kenos’ meaning hollow and ‘Sphaira’ meaning sphere [20]. They have a plethora of superior properties such as low density, high-temperature resistance, remarkable strength, high workability, high dispersibility.

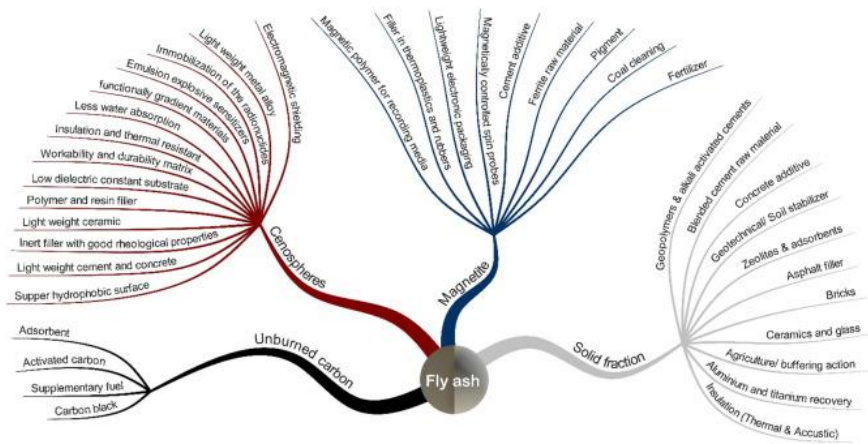


**Figure 2.** Utilization of flyash as cenospheres [7]

Thus, they are one of the most valuable by-products to be used as a filler in lightweight concrete. As cenospheres are the by-product of flyash, their concentration in flyash varies over a wide range. Also, their formation is dependent on the total mineral content of the coal used and the process of combustion. The use of cenospheres in cementitious materials has proved to be one of the promising materials for using it in structural applications.

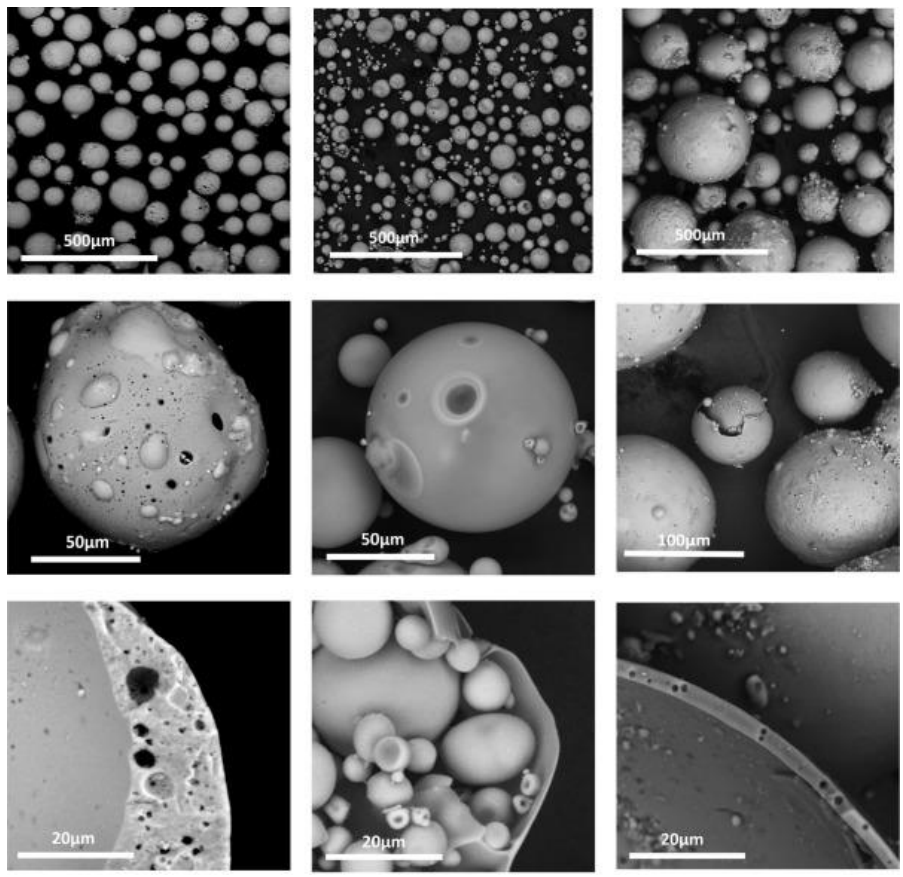


**Figure 3**. Scanning Electron Microscope (SEM) images of various types of cenosphere [21]

**Table 1.** Summary of cementitious materials using cenospheres in the previous studies

| Authors | Water to cement ratio | Size of cenospheres (μm) | Cenospheres content | Characteristics of mix type | 28-days Compressive strength (MPa) |
|---|---|---|---|---|---|
| [22] | 0.3-0.7 | 50-400 | 0-70 % wt. of the binder | Fiber reinforced | 30.38-55.92 |
| [13] | 0.5 | 94 | 0-25% wt. of the binder | Magnesium oxychloride cement | 64.30-94.60 |
| [12] | 0.35,0.27 | 106 | 50% vol of the mixture | Fine and coarse aggregates in a concrete | 54.28-60.67 |
| [23] | 0.3 | 1500-2000 | 0-50% vol of the mixture | Concrete | 5.04-33.03 |
| [24] | 0.43 | 106,160,600 | 0-28% vol of the mixture | Mortar | 35.40-62.75 |
| [14] | 0.32 | 100.732 | 0-0.3% wt. of the binder | Fiber reinforced (PVA fiber) | 63.94-70.69 |
| [25] | 0.5 | 150-300 | 0-100% vol of the concrete | FAC replaced natural coarse aggregate in cement concrete | 25-37.70 |
| [26] | 0.29-0.68 | 56.3, 834, 117.5 | Not available | Cement paste | 25.40-55.10 |
| [27] | 1.2* | 100-320 | Not available | *FAC to water ratio-1.2 | 0.55-2.88 |
| [18] | 0.26 | 200 | 60 & 100% vol of the mixture | Green lightweight Engineered cementitious composites which used iron ore tailings, flyash, and flyash cenosphere | 44.3-48.1 |

## 2.3. Performance of cenospheres on mechanical and physical properties in cementitious materials

### 2.3.1. Mechanical properties

Compressive strength is the index for determining other properties as well. It is also a widely researched property for cementitious materials because other properties such as flexural strength, splitting tensile strength, etc. are dependent on this property. It is one of the prominent properties that indicate holistic performance.

Water to cement content has a significant effect on the compressive strength of concrete. Lower the water to cement ratio, the higher the compressive strength. The study by Zhou and Brooks et al., 2019 [12], Huang et al., 2013 [18] have used the lowest water to cement ratio, 0.3 and 0.26, respectively with small size cenospheres ranging from 100 µm to 200 µm. In the study by Brooks et al., 2018 [24], it was reported that compressive strength followed an increasing trend with the incorporation of a smaller size of 106 µm and 160 µm. Also, it was found that compressive strength increased up to a content of 21% cenospheres by the volume of the mixture. Similarly, the compressive strength was found to decrease with the incorporation of a bigger size cenosphere i.e. 600 µm. The reasons for the decrement in compressive strength were attributed to the increment of air voids content which was resulted because of the incorporation of cenospheres.

However, studies above by [14, 22-24, 26] reported a reduction in the compressive strength when cenospheres were used in concrete, mortar, paste, fiber reinforced concrete, engineered cementitious composites, and magnesium oxychloride cement, respectively.

To achieve low density, Lightweight concrete is produced using lightweight aggregates/fillers which have a lower density than normal aggregates. Cenospheres, used as a lightweight filler in cementitious materials, help to reduce the density of the material. The study of Brooks et al., 2018 [24], McBride et al., 2002 [28], Wu et al., 2015 [9], have reported that the density of the materials decreased with the increasing content of cenospheres. The reduction in density can be attributed to the lower density of the cenospheres whose density range from 618-908 kg/$m^3$.

### 2.3.2. Thermal Properties

Thermal conductivity is one of the properties of lightweight concrete which can absorb heat. Meaning that the concrete having lower thermal conductivity is not able to absorb heat and for hot regions, it can maintain the temperature and saves energy costs. The study by Brooks et al., 2018 [24], Wang et al., 2011 [29] investigated that thermal conductivity decreased with the decrease in density of the concrete. This means that higher content of cenospheres content in the concrete reduced thermal conductivity. The increase of void content created due to spherical morphology is equal for

reducing thermal conductivity and density of the lightweight concrete. Hence, while reducing the density of lightweight concrete, thermal insulation property of the concrete is also enhanced. It was reported that the sizes of cenospheres play a role in the reduction of thermal conductivity. As a result, the bigger size cenospheres have lower thermal conductivity than the smaller size of cenospheres because of more air void entrapped due to the larger size of cenospheres.

### 2.3.3. Durability properties

Porosity is one of the critical physical properties of concrete, which is required for measuring the durable properties of lightweight concrete. Porosity is the measurement of the volume of voids in concrete. Lightweight concrete contains voids as a result of the porous lightweight aggregates [30]. The total porosity is due to air voids porosity and lightweight aggregate porosity. Pores inside lightweight concrete are empty spaces inside the material and can be up to 67%.

There is a direct relationship between mechanical strength and density with porosity in the material. Porosity increases with the increasing amount of lightweight aggregates in the materials and simultaneously, decreases the compressive strength and density. There are various ways of measuring the porosity of lightweight concrete and some of them are as follows:

a. Vacuum saturation technique as per ASTM C-1202-12
b. Mercury Intrusion porosity
c. Micro-CT

Here in this study, the micro-CT technique has been used for the measurement of the inner microstructure of pores, pore volume, pore diameter, and porosity. This technique has very prominent advantages over other techniques which is a non-invasive method and is capable of internal analysis without damaging the specimen [31]. In the images obtained from micro CT, the spatial distribution of various components within the sample such as pores can be investigated in three dimensions which is easy to visualize. In addition to this, the segregation phenomenon was in the mix and quantification can be done. Other parameters of interest such as shape, size, and different micro solid phases in the microstructure can be explored using it. Along with the development of technology, it has become efficient to use for other several types of concrete such as lightweight aggregate, high-performance concrete, foamed, and porous concrete.

# Chapter 3. Materials and Methodology

## 3.1. Materials and mix proportions

Ingredients used in this study were white portland cement (WPC), undensified silica fume (SF) (Grade 940-U Elkem Materials), quartz powder (QP) (S-Sil 10 Micro silica, SAC Corporation, Korea), polycarboxylate based high-range water-reducing superplasticizer (SP) (Flow mix 3000U, Dongnam Co. Ltd., Korea) and cenospheres**.** The particle size distributions of WPC, QP, SF, and cenospheres were obtained through laser diffraction particle size analyzer (Horiba SZ-100Z, Horiba Ltd., Kyoto, Japan), the results of which are illustrated in **Figure 4 (b)**. The size of the cenospheres ranged from 10 to 100 μm with an average particle size of 52 μm. The true density of the cenospheres was 0.75 g/cm$^3$ as per the manufacturer. The X-ray diffraction analysis of the cenospheres showed that cenospheres mainly consisted of amorphous material with small amounts of quartz and mullite crystal (**Figure 4 (c)**).

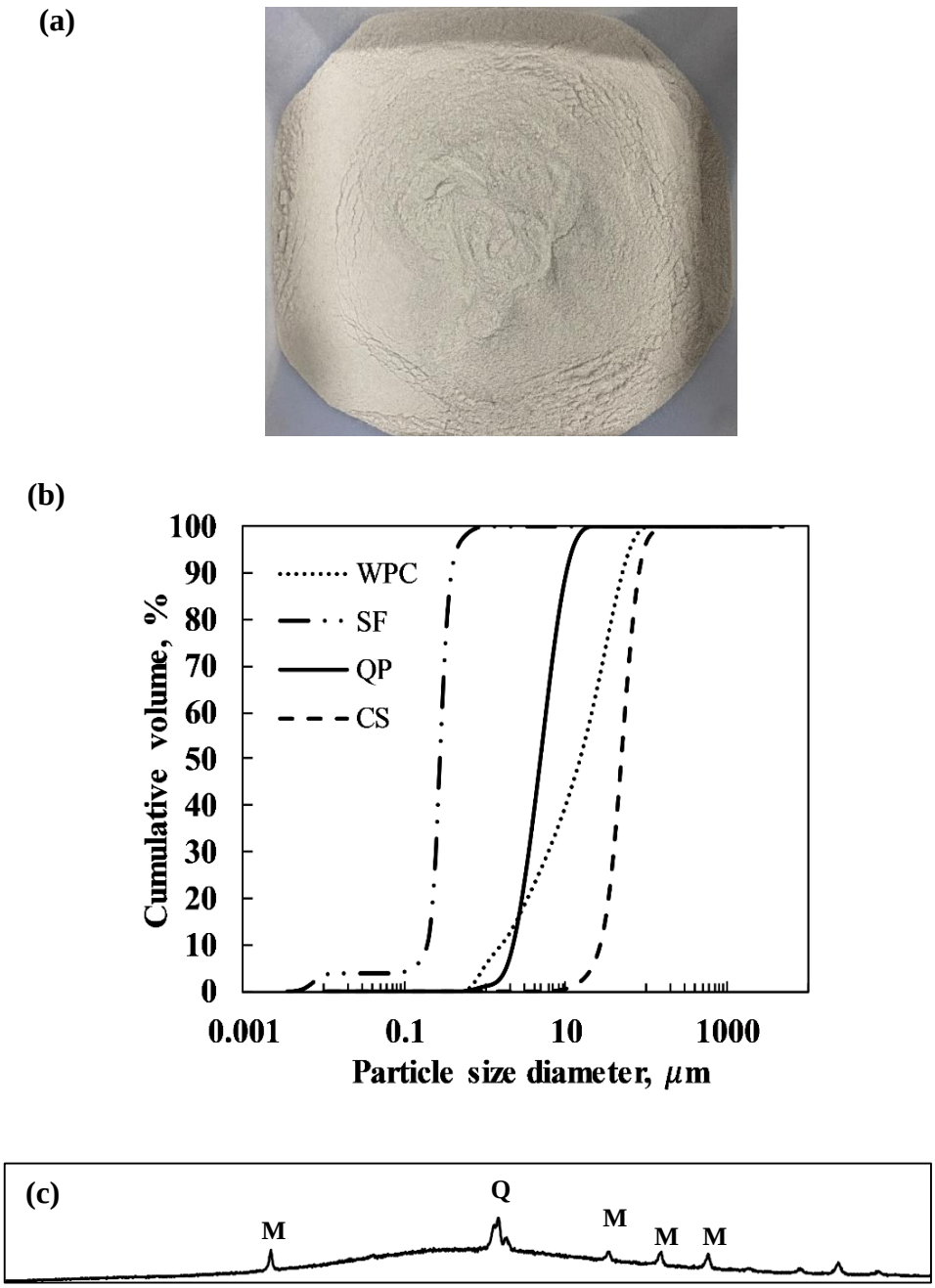


**Figure 4.** (a) Cenospheres used in this study (b) Particle size distribution of raw materials (c) X-ray diffraction pattern of cenospheres (M: Mulite; Q: Quartz)

The chemical composition of the raw materials were found via x-ray fluorescence (XRF) spectroscopy (S4 Pioneer, Bruker AXS GmbH, Germany), listed in **Table 2**. Three different mixes with varying cenospheres proportions (wt%) with a constant water-cement ratio of 0.23 were used **(Table 3).** The SP dosage was kept at 6% to maintain the workability of the mixture. The three mix type were cured at both ambient temperature (20 ºC and RH 60%) and heat treatment (90 ºC) to assess the strength development and characteristics of the cenospheres in the mix under different curing temperatures.

**Table 2.** Chemical composition (wt%) of ingredients

| Formula | $SiO_2$ | CaO | $Na_2O$ | $P_2O_5$ | $SO_3$ | $Al_2O_3$ | MgO | $Fe_2O_3$ | $TiO_2$ | $ZrO_2$ | $K_2O$ | MnO | Total |
|---|---|---|---|---|---|---|---|---|---|---|---|---|---|
| WPC | 15.38 | 73.64 | 0.28 | 0.06 | 4.21 | 3.54 | 2.07 | 0.41 | 0.08 | - | 0.15 | 0.05 | 99.87 |
| SF | 96.9 | 1.54 | 0.16 | 0.05 | - | 0.29 | 0.18 | 0.15 | 0.01 | - | 0.64 | 0.03 | 99.95 |
| QP | 97.7 | 1.37 | 0.02 | - | - | 0.49 | 0.21 | 0.05 | 0.08 | - | 0.02 | 0.01 | 99.95 |
| Cenosphere | 67.33 | 0.27 | 0.49 | 0.46 | 0.03 | 23.16 | 0.36 | 1.48 | 0.35 | 0.01 | 5.83 | - | 99.77 |

**Table 3.** Mix proportions by weight (%) of cement

| Mix id | Water, % | Cement, % | Silica fume, % | Quartz powder, % | Super-plasticizer % | Cenosphere, wt. % |
|---|---|---|---|---|---|---|
| CS0 | 23 | 100 | 25 | 35 | 6 | 0 |
| CS0-HT | 23 | 100 | 25 | 35 | 6 | 0 |
| CS10 | 23 | 100 | 25 | 35 | 6 | 10 |
| CS10-HT | 23 | 100 | 25 | 35 | 6 | 10 |
| CS20 | 23 | 100 | 25 | 35 | 6 | 20 |
| CS20-HT | 23 | 100 | 25 | 35 | 6 | 20 |

*CS10-HT – denotes the proportion of cenospheres in the mix which is 10 by wt% and the curing method was heat treatment at 90 $^{o}$C.

### 3.2. Mixing method, curing, and casting

The WPC, SF, and QP were mixed following the mixing method used by [32-34]. However, we mixed the mixture at least 10 minutes longer than the previous studies. The mixtures, that previous studies considered had silica sand which facilitated the dispersion of the other dry ingredients sufficiently. As this study mix proportion did not incorporate silica sand, required a longer time to get a well dispersed and homogeneous mixture. After mixing the dry ingredients, water and SP were mixed and poured into it. After which, it was mixed until liquid state. Then, cenospheres were added slowly until the cenospheres were fully dispersed in the mix [35]. Once the specimens are cast, they were covered immediately with plastic sheets to avoid evaporation. The specimens were demoulded after 72 hours because of the high amount of SP used that delayed the hydration process and hence, prolonged the demoulding time. The specimens were cured at 20 °C and 60% relative humidity until days of testing for ambient curing whereas, for heat treatment, demoulded specimens after three days were cured at 90 °C under sealed condition for 48 hours and after which, they were cured under the same conditions as an ambient condition until testing days.

### 3.3. Experimental method

#### 3.3.1. Mechanical and physical properties

The workability of the fresh mixture was measured using ASTM C230 [36]. The test consists of placing the fresh mix in a truncated conical mould on the flow table. After lifting the mould vertically, flow table was jolted 25 times and the final average spread diameter in two perpendicular directions was noted for measuring the flow value.

**Figure 5.** Compressive strength testing set up

For each mix type, cube specimens of size 50×50×50 $mm^3$ were prepared, 3 for each mix type testing at 3, 5, 14, 28 days, respectively. Compressive strength was measured following ASTM C 109 [37] and the average of three results were used for determining compressive strength. The

same cube specimens were used for determining the density of 28 days of curing using the water displacement method. The average value of three results was reported as density.

### 3.3.2. Thermal conductivity

Two slabs, each of size (L=100, b=25, h=100) mm for each mix type were prepared. Curing conditions were the same as mentioned above in the compressive strength. Thermal conductivity was measured using NETZSCH Heat Flow Meter (HFM 436/3/1) as shown in **Figure 6** and performed according to ASTM C518 [38]. In this study, Kapton sensor was placed in between the slabs of identical composition and was heated. TPS 2500s were used for the heat flux measurement. The power was varied in the range of 0.2 Watt - 0.4 Watt and the time was varied in between 20-40 seconds.


**Figure 6.** Thermal conductivity testing set up

### 3.2.3. XRD and TGA

XRD was performed to obtain mineralogical characteristics for 28 days of hydrated samples for each mix type using X-ray diffractometer (labz XRD-6000, shimadzu CO., TOKYO JAPAN) with cu-kα radiation (λ=1.5418a). Crystallography open database (cod) were used for analysing diffraction pattern of the hardened paste specimens. For stopping the hydration at a specified date, specimens were ground into powder and then, were soaked in isopropyl alcohol, washed with diethyl ether, and subsequently dried under 40 ºC [39, 40]. TGA was performed with DSC/TG system (SDT Q600, TA Instrument Ltd., Newcastle, DE, USA) within a $N_2$ environment under a heating rate of 10 K/min up to 1050 ºC.

### 3.2.4. Micro-computed tomography (Micro-CT)

Micro-CT is a tool used to identify the inner microstructure of the concrete without destroying the specimen [41]. For each mix type, (25 × 25) mm cylindrical specimens were prepared to visualize and examine the internal microstructure of the specimens. Moreover, this helps to evaluate the porosity/pore size distribution of specimens cured at ambient and heat treatment for 28 days. Micro-CT test was performed by a micro-computed tomography scanner (SkyScan 1272, Bruker, Belgium). To get enough transmission of X-ray through the samples, a 0.11mm Cu energy filter was

used with the optimal current 100 μA and voltage 100 kV. According to the size distribution (10~100 μm) of the cenospheres measured by the laser diffraction particle size analyser, micro-CT scanning resolution was selected as 8 μm/pixel (volume resolution was 256 $\mu m^3$/voxel), and 1471 2D raw images with the size of 2452×2452 pixels were obtained.

**Table 4.** Scanning condition for specimens

| Source Voltage, kV | Source Current, μA | Scanning time, Hours | Pixel Size, μm | Filter |
|---|---|---|---|---|
| 100 | 100 | 4 | 8/Pixel | Cu 0.1mm |

Image processing and pore analysis were performed by CTAN, 3D image analysis suite software provided by Bruker. The circular area with a diameter of 1000 pixels in the centre of the raw image was selected as the region of interest (ROI). Layers from 250 to 1250 layers to form the cylindrical volume of interest (VOI) with the actual size of 8000 μm × 8000 μm were selected. The pores in each image were separated from the background by threshold segmentation. The global threshold was selected by visual matching with greyscale image, the appropriate threshold can be set by shifting between and comparing the binary image and raw image. To eliminate the possible differences caused by different threshold selection, the same global threshold value was applied to all scanning specimens. The pores in the binary image were white, and the background was black. The geometric

parameters of all the pores, such as volume, volume-equivalent sphere diameter, and spatial position, were counted out for subsequent analysis. To visualize the distribution of cenospheres and pore, 3D Visualization suite software (CTVOX, Bruker, Belgium) was used to render the 3D volume.

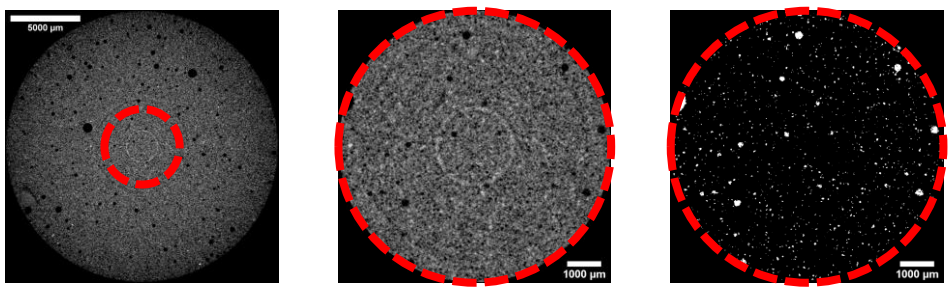


**(a)** **(b)** **(c)**

**Figure 7.** (a) 2D image of full tomographic reconstruction containing 10 % cenosphere (CS10). Red dotted area indicates the region for 3D reconstruction and further analysis, (b) Region of Interest (ROI), (c) Segmentation through threshold

#### *3.2.4.1. Process of quantification of micro-CT results*

For the quantification of micro-CT results, the volume of interest (VOI) of size 8000 µm × 8000 µm was chosen for all the mixes types that were scanned using micro-CT. VOI was divided into 8 blocks, each of size 1000 µm. For the volume of paste calculation, such as block 5 (**Figure 8**), the total volume of cenospheres (obtained from micro-CT processing) was subtracted from the total volume of block 5. The paste volume for each block was then, calculated following a similar process. A statistical equation: coefficient of variation (COV) was used to calculate the uniformity of paste volume in each block. The uniform distribution of paste volume in each block can indicate that cenospheres are uniformly distributed.

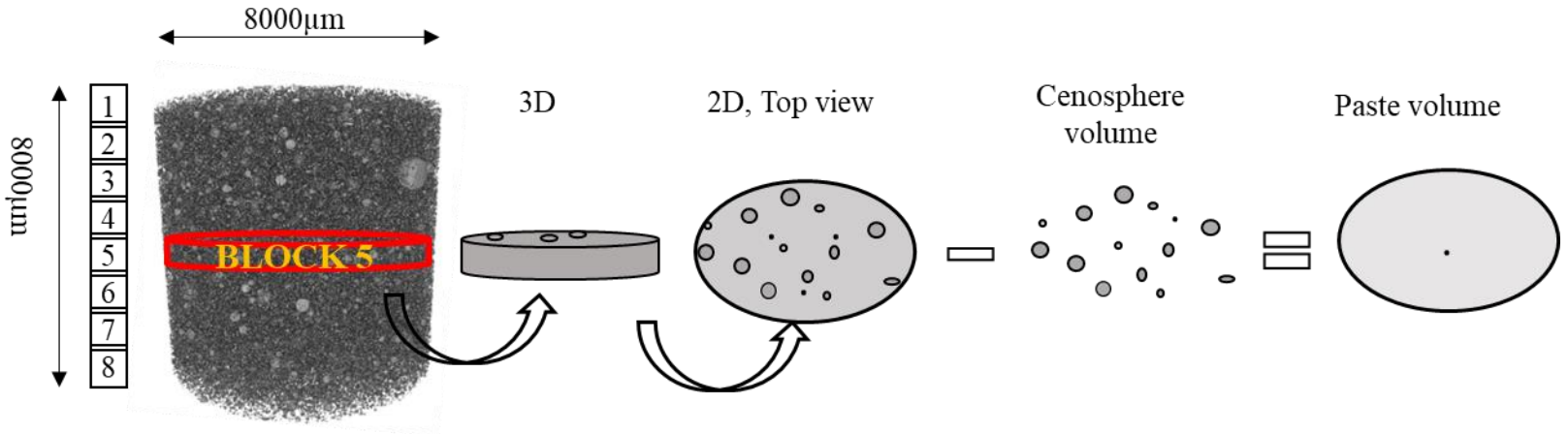


**Figure 8.** Schematic representation of the process of micro- CT results

# Chapter 4. Results and Discussions

## 4.1. Effect of cenospheres content on mechanical and physical properties

### 4.1.1. Workability

The flow of freshly prepared composites reduced from 280 mm to 250 mm when the cenospheres content increased from 10% to 20% (**Figure 9**). This reduction is because cenospheres may have absorbed water from the mix, which may have contributed to the reduction of workability. A similar result was reported by Patel et al., 2020 [25]. Besides, cenospheres increased the fineness of the mixture, which may have further reduced the flow.

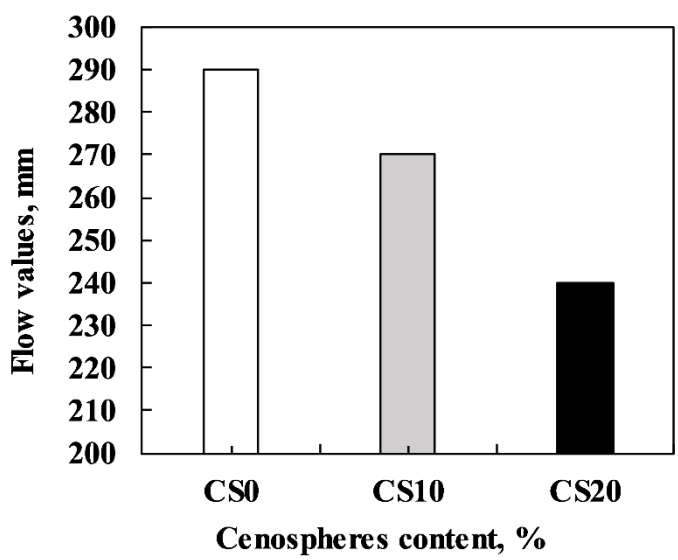


**Figure 9**. Flow at their fresh state

### 4.1.2. Compressive strength and density

When cenospheres content increased, the compressive strength of the composites reduced under both ambient and heat treatment (**Figure 10 (**a) and (b))**.** Similarly, the densities reduced with increasing cenospheres content. The reduction of compressive strength can be attributed to the increasing voids content, which decreased the bond strength between the binders: a similar phenomenon reported by [42]. Also, the reduction of the cementitious materials within the matrix which was replaced by cenospheres may have further contributed to this. Under heat treatment, a rapid increase of compressive strength was seen because of the accelerated pozzolanic reactions [43-45]. This resulted heat treated samples having higher compressive strength compared to the samples cured at ambient temperature. For heat treated samples, compressive strength was slightly decreased at 14 days and 28 days. In dense microstructures, the available space for subsequent hydration is limited which can cause micro-cracking for later age of hydration that can be to attributed for a slight decrease in strength at later ages [44, 45].

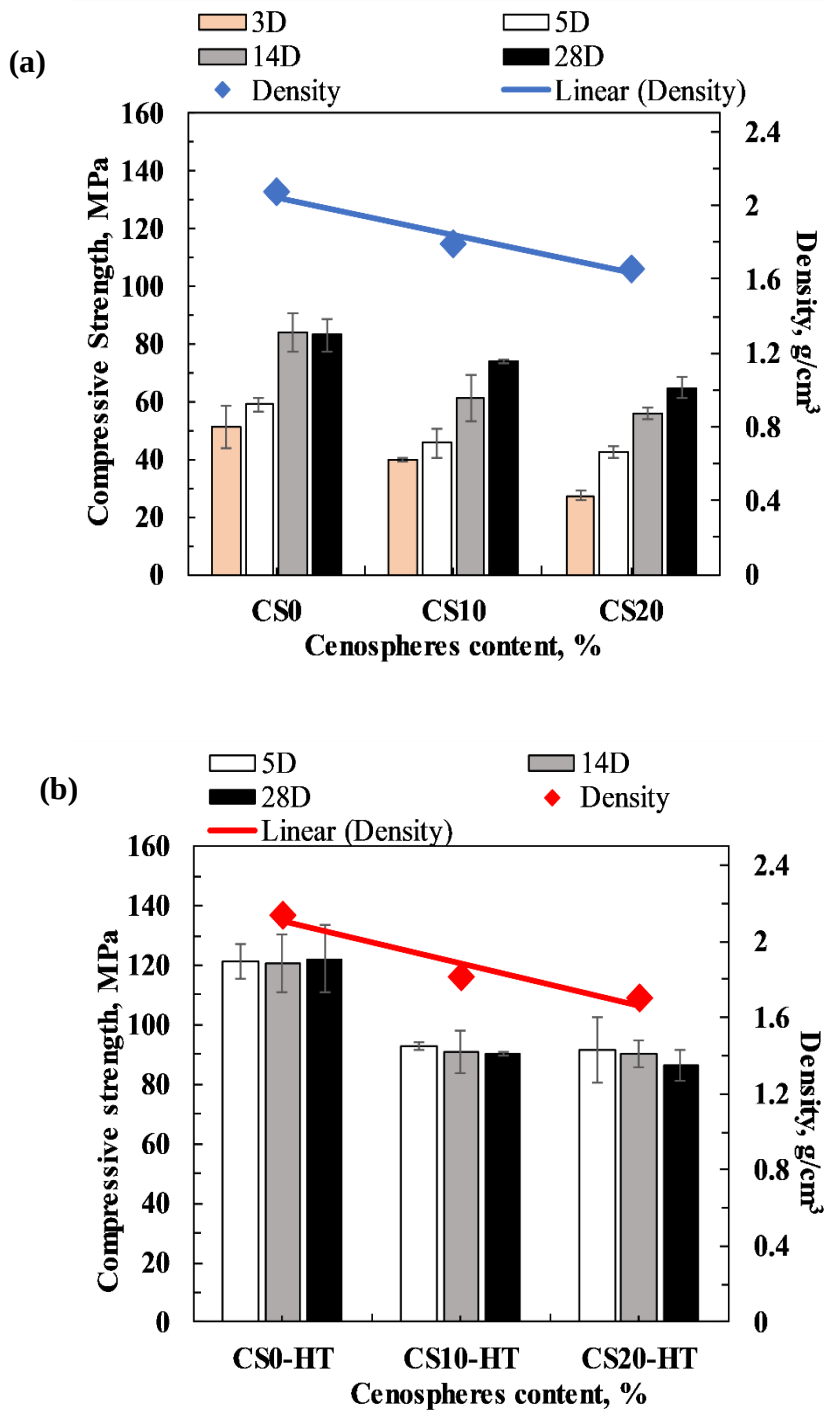


**Figure 10.** Compressive strength (a) ambient curing, (b) heat treatment

**Table 5**. Compressive strength and density values with standard deviation in the bracket

| Mix id | Compressive strength, MPa | | | | Density, $g/cm^3$ |
|---|---|---|---|---|---|
| | 3D | 5D | 14D | 28D | 28D |
| CS0 | 51.33 (7.33) | 58.93 (2.05) | 83.83 (6.85) | 83.17 (5.69) | 2.07 (0.022) |
| CS10 | 39.9 (0.43) | 45.56 (5.27) | 61.25 (7.81) | 74.03 (0.84) | 1.79 (0.019) |
| CS20 | 27.45 (1.69) | 42.48 (2.05) | 55.98 (2.08) | 64.81 (3.87) | 1.66 (0.043) |
| CS0-HT | 51.33 (7.33) | 121.12 (5.99) | 120.72 (9.85) | 122.03 (11.34) | 2.14 (0.024) |
| CS10-HT | 39.9 (0.43) | 92.49 (1.30) | 90.95 (7.21) | 90.08 (0.80) | 1.81 (0.053) |
| CS20-HT | 27.45 (1.69) | 91.44 (10.56) | 90.2 (4.63) | 86.52 (5.28) | 1.7 (0.013) |

Developed composites in this study demonstrated a higher compressive strength compared to previous studies (**Figure 11**) having similar densities. The water to cement ratio used in our study was much lower compared to other previous researches as reported in the study of Brooks et al., 2018 [24], Chen et al., 2020 [14], Zhou and Brooks et al., 2019 [12]. Further, the size of cenospheres used by those researchers was larger compared to this present study. The larger size of cenospheres exhibited an increase in air voids content yielding from the incorporation of the larger size cenospheres and resulted in decreasing compressive strength. Patel et al., 2020 [25], Wang et al., 2014 [26], Hanif et al., 2017 [22], Blanco et al., 2000 [23], also reported much lighter density using cenospheres, however, their compressive strength was much lower because of high cenospheres content and water to cement ratios. Hence, the lightweight composites developed in this study have substantially higher compressive strength for structural applications.

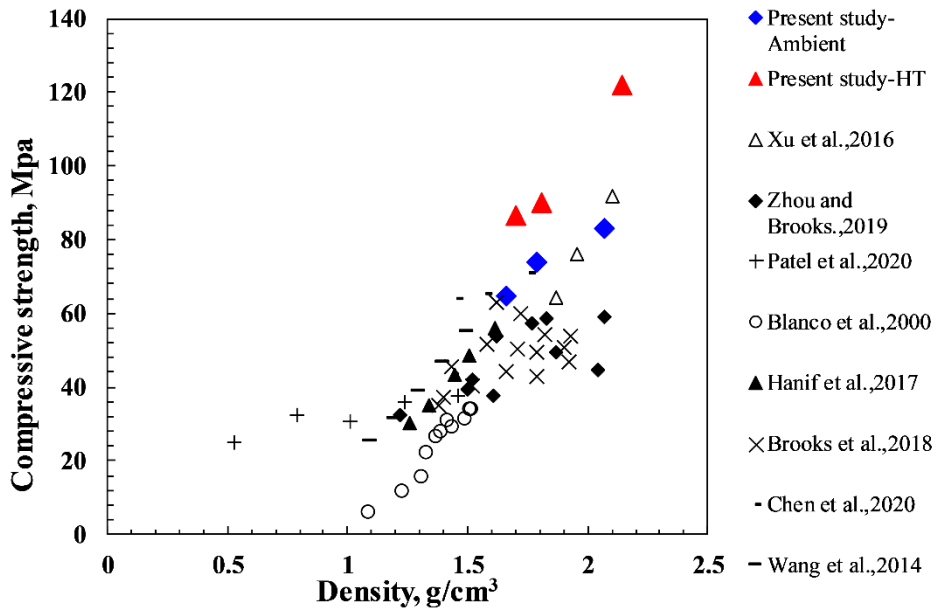


**Figure 11.** Comparison of present work with the previous works using cenospheres in terms of compressive strength [12-14, 22-26]

### 4.1.3. Thermal conductivity

Thermal conductivity decreased with decreasing density of the matrix (**Figure 12**). Due to the spherical morphology of the cenospheres, they help to create more voids content in the matrix Ultimately, this leads to more air getting entrapped in the specimens that lowered thermal conductivity [24]. Heat treatment, as expected, created denser microstructures. As a result, a slightly higher value of thermal conductivity for heat treated samples was observed. Therefore, a good linear relationship of density and thermal conductivity was observed which has also been explored and reported in the

literatures [4, 46, 47].

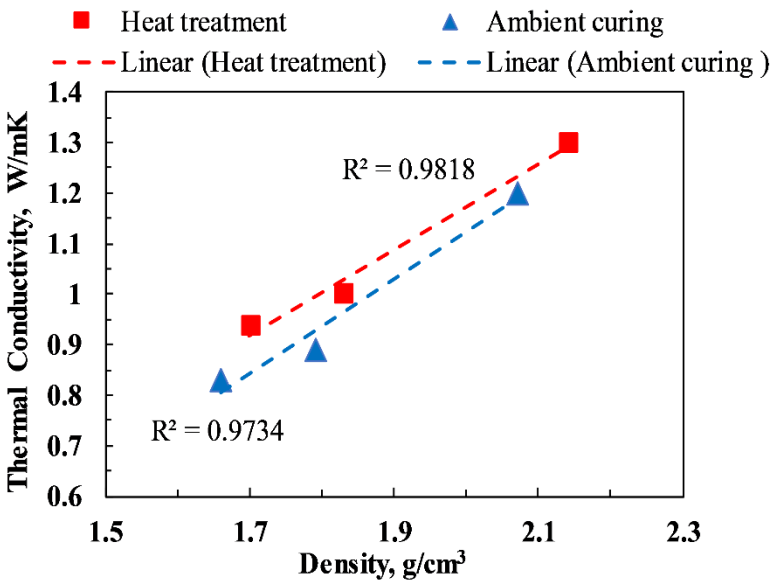


**Figure 12.** Effects of density on thermal conductivity for 28 days of curing

Similarly, the composites developed in this study showed higher compressive strength with low thermal conductivity illustrated in **Figure 13**. In the study of Brooks et al., 2018 [24], having a similar density range with our present study (**Figure 11**) showed higher thermal conductivities, because the mix type used was mortar. The presence of silica sand used in their mix type, which inherently has a higher conductivity, may have resulted in high thermal conductivity. Xu et al., 2016 [13], despite having high strength, high thermal conductivity was observed. The mix type used was magnesium oxychloride cement (MOC) that was chemically fabricated and applications

of MOC are still not widespread because of its poor water resistance. Hanif et al., 2014 [22], Losiewicz et al., 1996 [27], reported much lower thermal conductivities that could be resulting from very large sizes of cenospheres used in their studies compared to the present study.

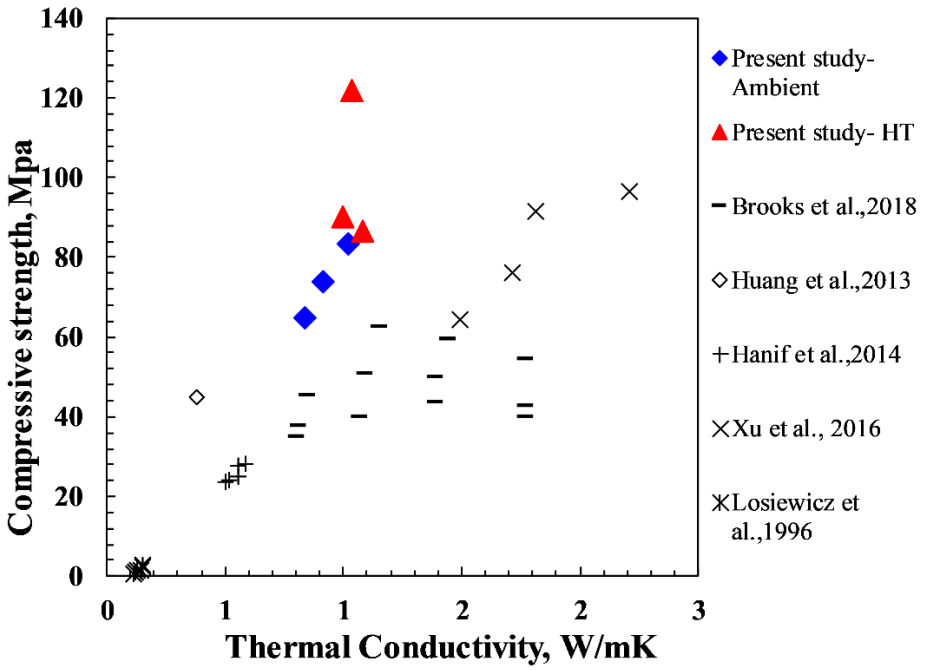


**Figure 13.** Comparison of present work with the previous works using cenospheres in terms of thermal conductivity [13, 18, 22, 24, 27]

### 4.2. XRD and TGA

XRD analysis results cured at 28 days for all the mix are shown in **Figure 14**. It was found that the peak corresponding to portlandite (main hydration product) decreased in heat treated samples. Furthermore, the peak

corresponding to ettringites disappeared and clinker minerals i.e., Alite ($C_3S$), Belite ($C_2S$) decreased in heat treated samples. The accelerated pozzolanic reaction caused due to heat treatment, led to more hydration product formation, and thus, decreasing the peak of portlandite and clinker minerals. Similar observations were made in the studies by [44, 48-52]. Other than that, no other additional product formation or chemical reaction was observed with the inclusion of cenospheres.

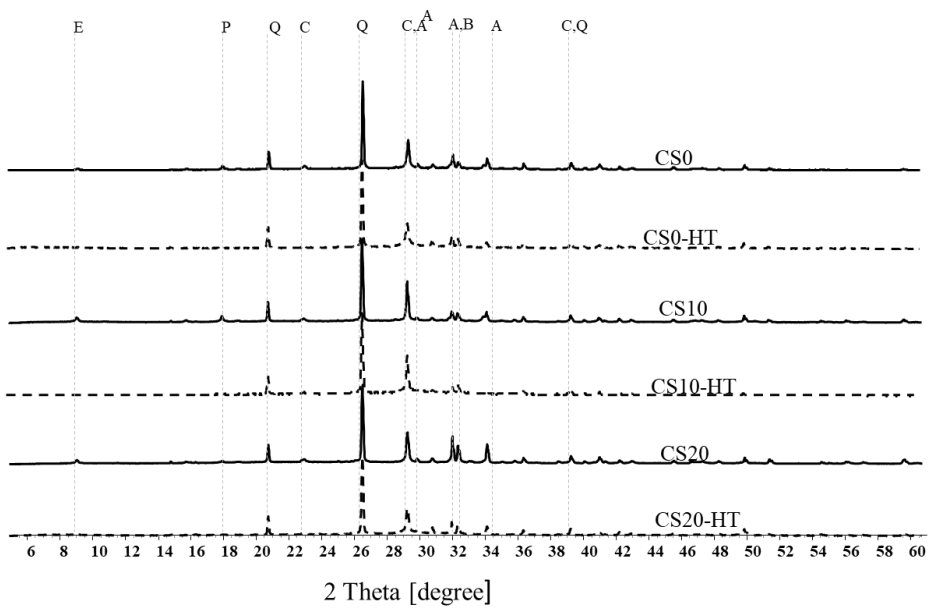


**Figure 14**. XRD pattern of 28 days cured specimens. (A: alite; B: belite; C: calcite; E: ettringite; P: portlandite; Q: quartz)

Qualitative TG analysis of the specimens as a function of temperature ranging from room temperature to 1100 ºC is presented in **Figure 15**.

Portlandite, which decomposed between 400~500 °C disappeared with the heat treatment that confirmed the mineralogical changes observed by XRD pattern. Further, Calcite ($CaCO_3$) which decomposed in the range of 600~800 °C found to have main weight loss. The weight loss around 800 ºC to 1100 ºC, showed higher irregularities. This is because the small amount of sample weight used for the analysis, might have affected the results at these temperatures. Thus, cenospheres were not found to be involved in any chemical reactions as demonstrated by TGA.

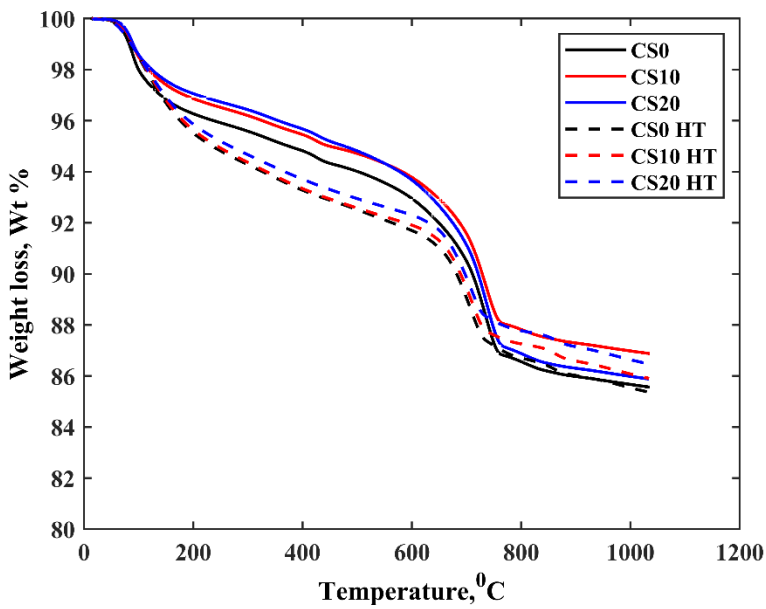


**Figure 15.** TGA results of 28 days cured specimens

### 4.3. Tomographic analysis

3D volume rendering of the isolated pores and cenospheres with their distribution in VOI was performed as shown in **Figures 16** and **17**. Size ranging from 10 to 100 µm were separated as pores whereas voids size smaller than 10 µm and greater than 10 µm were classified as noise and air voids, respectively. From 3D visual inspection of rendered images of the isolated cenospheres in all mix types, it indicated that the cenospheres in the matrix were well distributed accordingly to the increase of cenospheres content implying no segregation phenomena in the chosen mix design. Thus, it verified the homogeneity throughout VOI. This could be achieved due to low water-cement ratio used in the mix proportion enabling the paste to be thick and viscous enough to prevent cenospheres segregation. Thereafter, further microstructural analysis was performed.

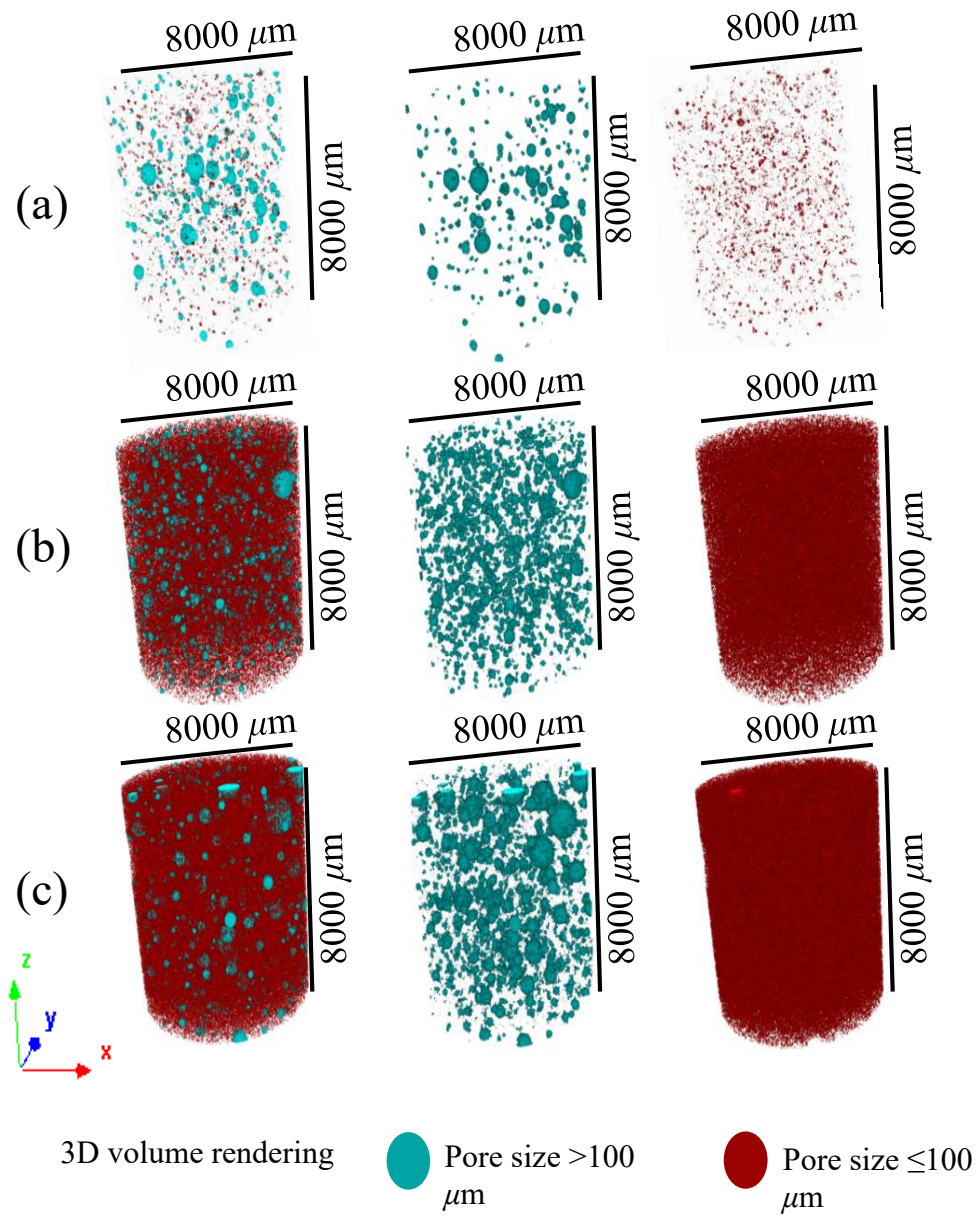


**Figure 16.** 3D rendering image of specimens after 28 days of ambient curing (a) CS0, (b) CS10, (c) CS20

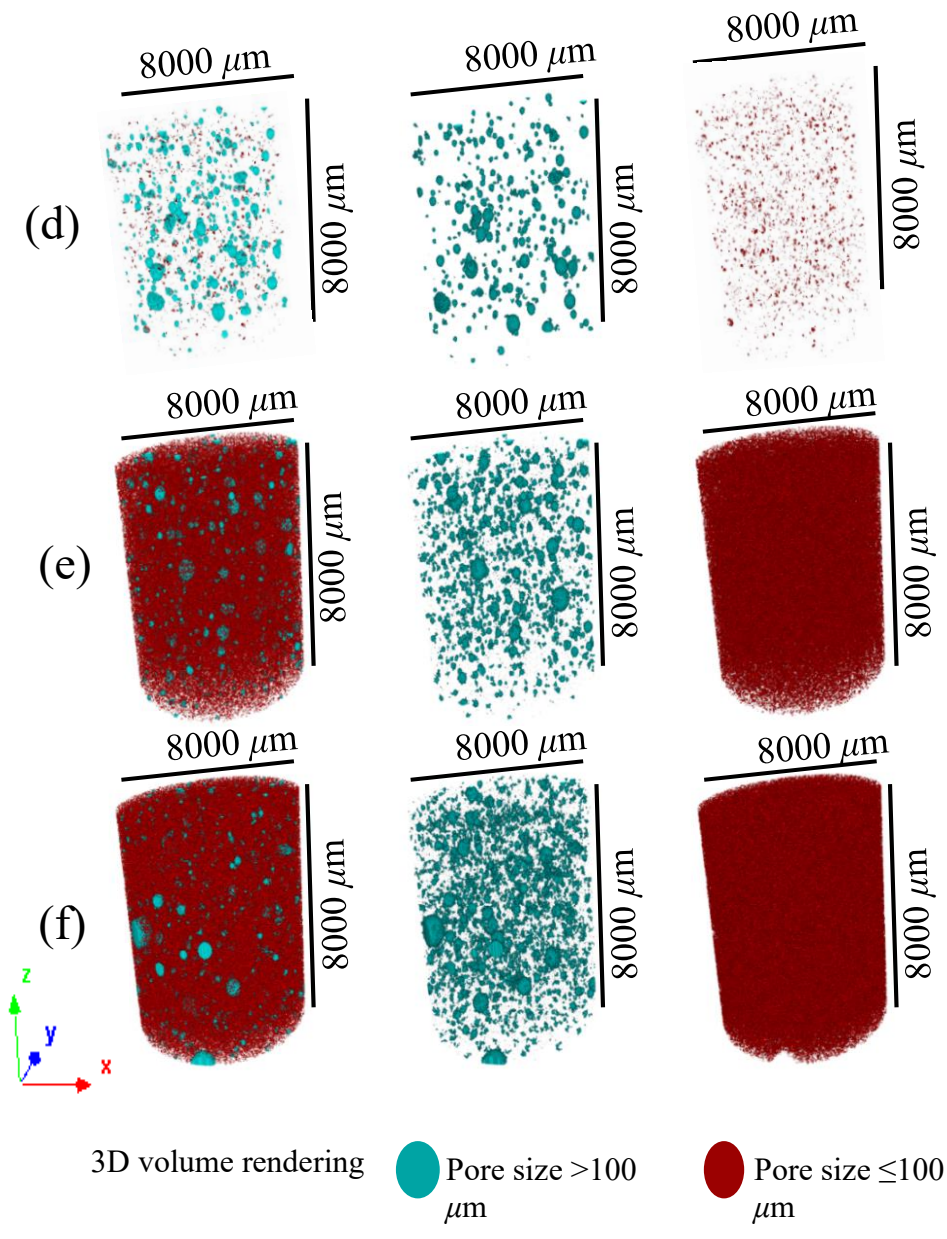


**Figure 17.** 3D rendering image of specimens after 28 days of heat treatment

(c) CS0-HT, (d) CS10-HT, (e) CS20-HT

### 4.3.1. Quantification of micro-CT data

To verify the uniform distribution of the cenospheres in the mix from the obtained results of micro-CT image analysis, a volumetric fraction of the paste throughout the volume of interest (VOI) was calculated. To calculate paste volume, the volume of cenospheres obtained from micro-CT results from the volume of each block was subtracted [5]. For uniformity of paste volume in each block, a mathematical-statistical tool called the coefficient of variation (COV) defined by equation (1) was used.

$$COV = \frac{standard\ deviation}{Mean} \times 100\% \quad (1)$$

COV for CS0, CS10, CS20, CS0-HT, CS10-HT and CS20-HT was 0.31%, 0.23%, 1.30%, 0.33%, 0.25%, 0.48%, respectively. COV was increased with the increase of cenospheres content, but this value is still low, indicating that the paste was uniformly distributed along VOI. **Figure 18 (a)** and **(b)** are the graphical indications of the ratio of paste volume to the total volume per block which indicated the dispersion of cenospheres in the mix was relatively uniform and hence, implied that there is no floatation effect of cenospheres in the mix.

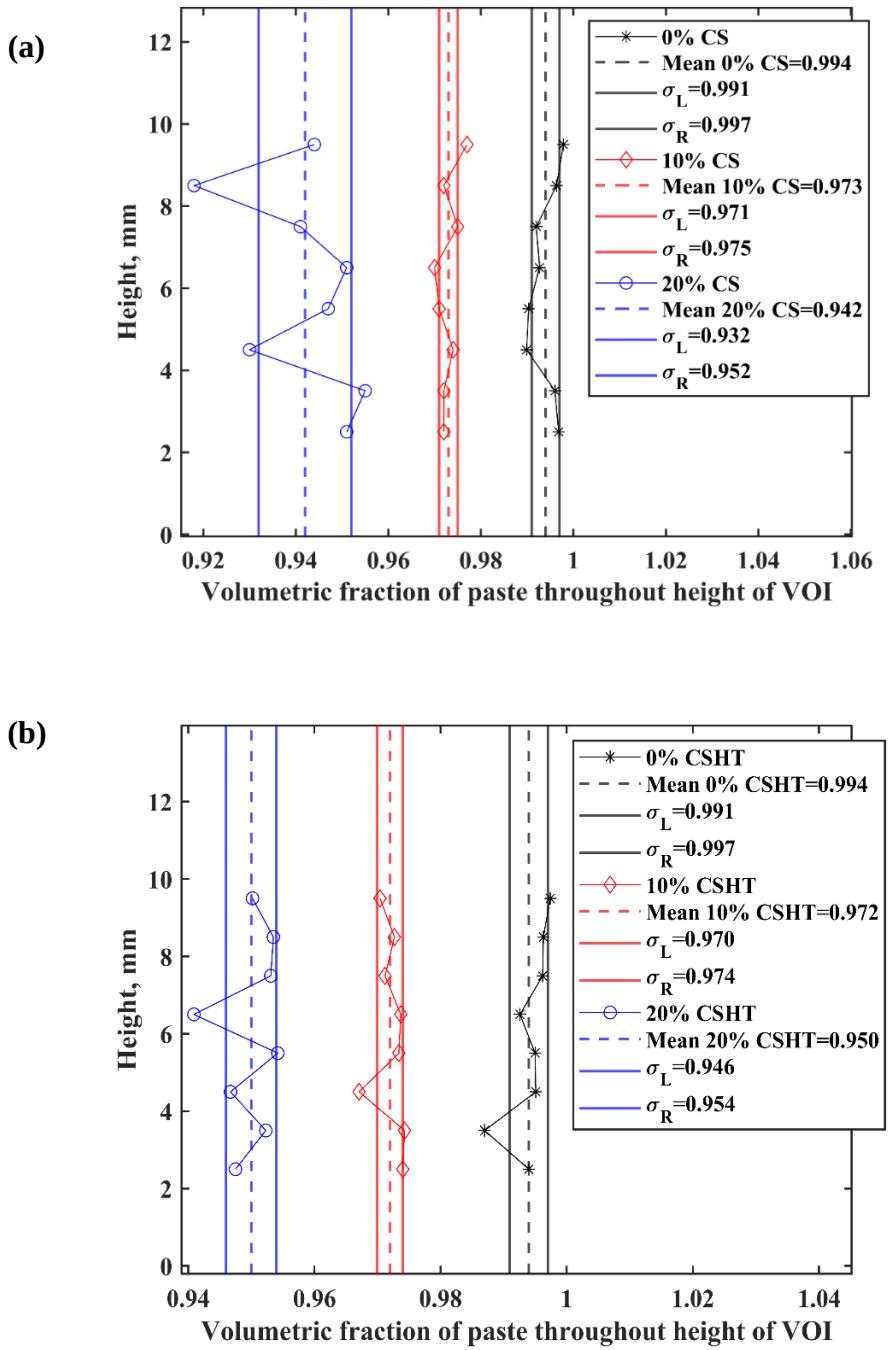


**Figure 18.** Volumetric fraction of paste throughout VOI height (a) CS0, CS10, CS20 (b) CS0-HT, CS10-HT, CS20-HT

### 4.3.2. Porosities

The cumulative porosities distribution of the cenospheres composites after 28 days of curing, suggested that porosity increased with the addition of cenospheres content (**Figure 19 (a)** and **(b)**). The results illustrated that a consistent increase of cenospheres addition in the composites led to porosity increment. Additionally, based on the threshold pore diameter, porosities due to air voids and due to cenospheres were calculated. Hence, it helped to calculate individual contributions to porosity separately with these entities.

**(a)**

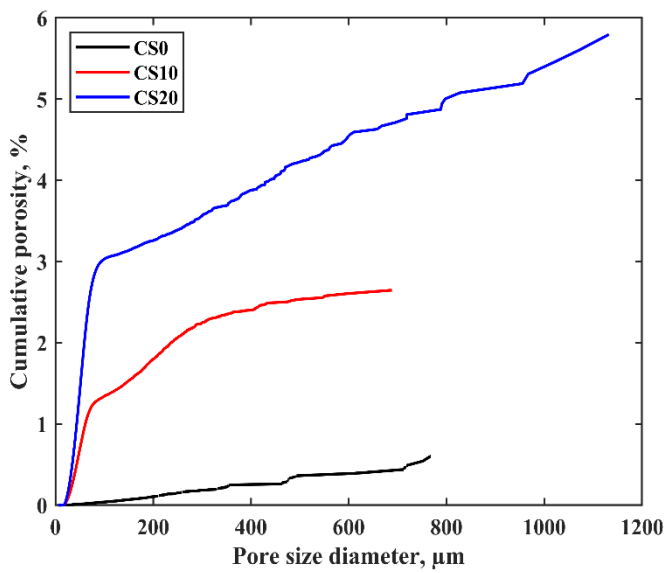

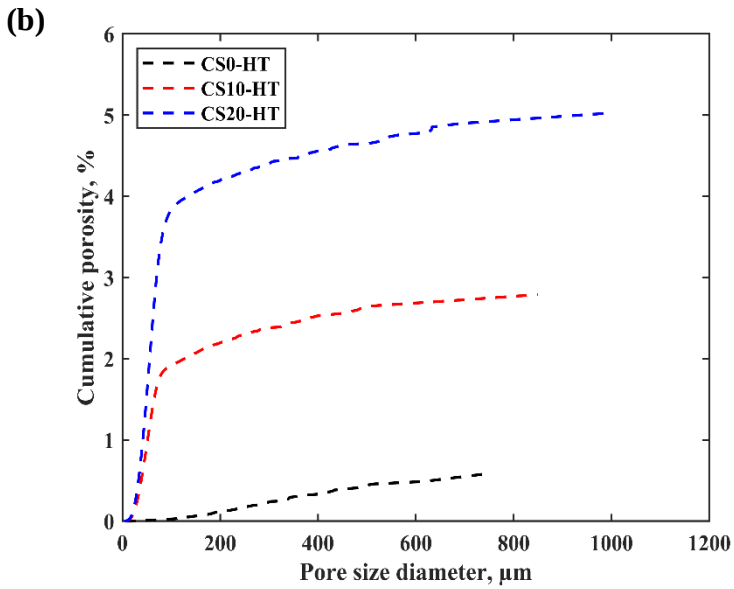


**Figure 19.** Cumulative porosities of specimens after 28 days of curing (a) ambient curing (b) heat curing

According to the findings, porosity attributable to air voids were lower than that attributable to cenospheres in all mix type, except for CS10 as shown in (**Figure 20**)**.** It could be noted that while choosing and cropping VOI, cenospheres may have cropped or some of it may have broken while mixing. This may have resulted in a slight decrement of porosity due to cenospheres. However, it is noteworthy that an increasing trend for porosities due to air voids and cenospheres was observed when the cenosphere content increased. The lower porosity was observed for heat treated samples compared to ambient curing, similar as reported by [53]. This could be because at high

temperature, the formation of hydration products increased and hence, porosity decreased.

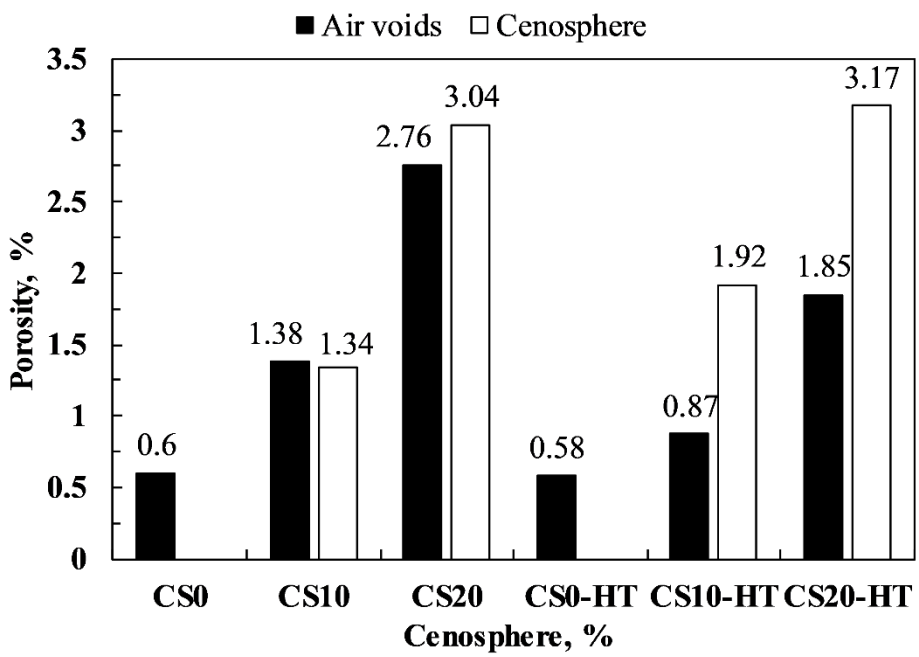


**Figure 20.** Porosities due to air voids and cenospheres

# Chapter 5. Conclusion

Mechanical and physical properties of high strength and lightweight cementitious composites using cenospheres were investigated with varying cenospheres content and different curing temperatures. Based on the results of this study, the following conclusions were drawn

1. Compressive strength, density, and thermal conductivity decreased with the increment of cenospheres content. However, the developed composites in the present study showed higher compressive strength while maintaining lower density and lower thermal conductivity compared to values reported in other previous studies.

2. Micro-CT results indicated that the problem of segregation in lightweight concrete was not observed. Cenospheres were well dispersed in the mix and the mixtures were relatively homogeneous.

3. XRD and TGA analysis showed that the cenospheres do not show chemical reactivity in the adopted mix design used in the present study.

4. There is a possibility of using the developed composites in the structures exposed to saline environments due to their low porosities.

The size of cenospheres also plays an important role in determining strength. Hence, further research may be carried out on the different sizes of cenospheres for a better understanding of cenospheres in low-density concrete and also for examining the chemical reactivity of cenospheres in the mix.

# References

[1] S. Chandra, L. Berntsson, Lightweight aggregate concrete, Elsevier2002.

[2] "A. Committee, 213, ACI 213R-03 Guide for Structural Lightweight-Aggregate Concrete", 2009.

[3] H. Uysal, R. Demirboğa, R. Şahin, R. Gül, "The effects of different cement dosages, slumps, and pumice aggregate ratios on the thermal conductivity and density of concrete", Cement and Concrete Research 34(5) (2004) 845-848.

[4] İ.B. Topçu, T. Uygunoğlu, "Properties of autoclaved lightweight aggregate concrete", Building and Environment 42(12) (2007) 4108-4116.

[5] M. Mohammad, E. Masad, T. Seers, S.G. Al-Ghamdi, "Properties and Microstructure Distribution of High-Performance Thermal Insulation Concrete", Materials (Basel) 13(9) (2020).

[6] O. Sengul, S. Azizi, F. Karaosmanoglu, M.A. Tasdemir, "Effect of expanded perlite on the mechanical properties and thermal conductivity of lightweight concrete", Energy and Buildings 43(2-3) (2011) 671-676.

[7] N. Ranjbar, C. Kuenzel, "Cenospheres: A review", Fuel 207 (2017) 1-12.

[8] S. White, E. Case, "Characterization of fly ash from coal-fired power plants", Journal of Materials Science 25(12) (1990) 5215-5219.

[9] Y. Wu, J.-Y. Wang, P.J.M. Monteiro, M.-H. Zhang, "Development of ultra-lightweight cement composites with low thermal conductivity and high specific strength for energy efficient buildings", Construction and Building Materials 87 (2015) 100-112.

[10] J. Ding, S. Ma, S. Shen, Z. Xie, S. Zheng, Y. Zhang, "Research and industrialization progress of recovering alumina from fly ash: A concise review", Waste Management 60 (2017) 375-387.

[11] A. Adesina, "Sustainable application of cenospheres in cementitious materials – Overview of performance", Developments in the Built Environment 4 (2020).

[12] H. Zhou, A.L. Brooks, "Thermal and mechanical properties of structural lightweight concrete containing lightweight aggregates and fly-ash cenospheres", Construction and Building Materials 198 (2019) 512-526.

[13] B. Xu, H. Ma, C. Hu, Z. Li, "Influence of cenospheres on properties of magnesium oxychloride cement-based composites", Materials and Structures 49(4) (2016) 1319-1326.

[14] W. Chen, Z. Qi, L. Zhang, Z. Huang, "Effects of cenosphere on the mechanical properties of cement-based composites", Construction and Building Materials 261 (2020).

[15] B. Chandra, "Lightweight Aggregate Concrete".

[16] R. Muralitharan;, V. Ramasamy, "Basic Properties of Pumice Aggregates", International Journal of Earth Sciences and Engineering Vol. 08 (2015) 256-258.

[17] T. Gao, B.P. Jelle, A. Gustavsen, S. Jacobsen, "Aerogel-incorporated concrete: An experimental study", Construction and Building Materials 52 (2014) 130-136.

[18] X. Huang, R. Ranade, Q. Zhang, W. Ni, V.C. Li, "Mechanical and thermal properties of green lightweight engineered cementitious composites", Construction and Building Materials 48 (2013) 954-960.

[19] A. Dixit, S.D. Pang, S.-H. Kang, J. Moon, "Lightweight structural cement composites with expanded polystyrene (EPS) for enhanced thermal insulation", Cement and Concrete Composites 102 (2019) 185-197.

[20] S. Torrey, Coal Ash Utilization: Fly Ash, Bottom Ash, and Slag, Noyes Data Corporation1978.

[21] S. Kristombu Baduge, P. Mendis, R. San Nicolas, K. Nguyen, A. Hajimohammadi, "Performance of lightweight hemp concrete with alkali-activated cenosphere binders exposed to elevated temperature", Construction and Building Materials 224 (2019) 158-172.

[22] A. Hanif, Z. Lu, S. Diao, X. Zeng, Z. Li, "Properties investigation of fiber reinforced cement-based composites incorporating cenosphere fillers", Construction and Building Materials 140 (2017) 139-149.

[23] F. Blanco, P. García, P. Mateos, J. Ayala, "Characteristics and properties of lightweight concrete manufactured with cenospheres", Cement and Concrete Research 30(11) (2000) 1715-1722.

[24] A.L. Brooks, H. Zhou, D. Hanna, "Comparative study of the mechanical and thermal properties of lightweight cementitious composites", Construction and Building Materials 159 (2018) 316-328.

[25] S.K. Patel, H.P. Satpathy, A.N. Nayak, C.R. Mohanty, "Utilization of Fly Ash Cenosphere for Production of Sustainable Lightweight Concrete", Journal of The Institution of Engineers (India): Series A 101(1) (2019) 179-194.

[26] J.-Y. Wang, Y. Yang, J.-Y.R. Liew, M.-H. Zhang, "Method to determine mixture proportions of workable ultra lightweight cement composites to

achieve target unit weights", Cement and Concrete Composites 53 (2014) 178-186.

[27] M. Losiewicz, D.P. Halsey, S.J. Dews, P. Olomaiye, F.C. Harris, "An investigation into the properties of micro-sphere insulating concrete", Construction and Building Materials 10(8) (1996) 583-588.

[28] S.P. McBride, A. Shukla, A. Bose, "Processing and characterization of a lightweight concrete using cenospheres", Journal of Materials Science 37(19) (2002) 4217-4225.

[29] M.-R. Wang, D.-C. Jia, P.-G. He, Y. Zhou, "Microstructural and mechanical characterization of fly ash cenosphere/metakaolin-based geopolymeric composites", Ceramics International 37(5) (2011) 1661-1666.

[30] M. Kurpińska, T. Ferenc, "Effect of porosity on physical properties of lightweight cement composite with foamed glass aggregate", ITM Web of Conferences 15 (2017) 06005.

[31] S.-Y. Chung, J.-S. Kim, D. Stephan, T.-S. Han, "Overview of the use of micro-computed tomography (micro-CT) to investigate the relation between the material characteristics and properties of cement-based materials", Construction and Building Materials 229 (2019) 116843.

[32] S.-H. Kang, S.-G. Hong, J. Moon, "Importance of drying to control internal curing effects on field casting ultra-high performance concrete", Cement and Concrete Research 108 (2018) 20-30.

[33] S.-H. Kang, S.-G. Hong, J. Moon, "Shrinkage characteristics of heat-treated ultra-high performance concrete and its mitigation using superabsorbent polymer based internal curing method", Cement and Concrete Composites 89 (2018) 130-138.

[34] S.-H. Kang, S.-G. Hong, J. Moon, "The use of rice husk ash as reactive filler in ultra-high performance concrete", Cement and Concrete Research 115 (2019) 389-400.

[35] N. Lee, J. Pae, S-H. Kang, H. Kim, J. Moon, Development of high strength and lightweight cementitious composites using hollow glass micropshere in a low water-to-cement matrix, in: S.N. University (Ed.) 2021.

[36] A. C230, "Standard specification for flow table for use in tests of hydraulic cement,West Conshohocken (PA):ASTM Interanational ", (2002).

[37] A. ASTM, "Standard test method for compressive strength of hydraulic cement mortars (using 2-in. or [50-mm] cube specimens)", Annual

Book of ASTM StandardsAnnual Book of ASTM Standards 4(1) (2013) 1-9.

[38] "C. ASTM,177/C518. 2004, Standard Test Method for Steady-State Thermal Transmission Properties by Means of the Heat Flow Meter Apparatus".

[39] R. Snellings, J. Chwast, Ö. Cizer, N. De Belie, Y. Dhandapani, P. Durdzinski, J. Elsen, J. Haufe, D. Hooton, C. Patapy, M. Santhanam, K. Scrivener, D. Snoeck, L. Steger, S. Tongbo, A. Vollpracht, F. Winnefeld, B. Lothenbach, "Report of TC 238-SCM: hydration stoppage methods for phase assemblage studies of blended cements—results of a round robin test", Materials and Structures 51(4) (2018) 111.

[40] J. Zhang, G.W. Scherer, "Comparison of methods for arresting hydration of cement", Cement and Concrete Research 41(10) (2011) 1024-1036.

[41] S.-Y. Chung, M.A. Elrahman, D. Stephan, P.H. Kamm, "The influence of different concrete additions on the properties of lightweight concrete evaluated using experimental and numerical approaches", Construction and Building Materials 189 (2018) 314-322.

[42] H.P. Satpathy, S.K. Patel, A.N. Nayak, "Development of sustainable lightweight concrete using fly ash cenosphere and sintered fly ash aggregate", Construction and Building Materials 202 (2019) 636-655.

[43] N. Lee, Y. Jeong, H. Kang, J. Moon, "Heat-Induced Acceleration of Pozzolanic Reaction Under Restrained Conditions and Consequent Structural Modification", Materials 13(13) (2020) 2950.

[44] S.-H. Kang, J.-H. Lee, S.-G. Hong, J. Moon, "Microstructural Investigation of Heat-Treated Ultra-High Performance Concrete for Optimum Production", Materials 10(9) (2017) 1106.

[45] H. Kang, N. Lee, J. Moon, "Elucidation of the Hydration Reaction of UHPC Using the PONKCS Method", Materials 13(20) (2020) 4661.

[46] R. Gül, E. Okuyucu, İ. Türkmen, A.C. Aydin, "Thermo-mechanical properties of fiber reinforced raw perlite concrete", Materials Letters 61(29) (2007) 5145-5149.

[47] R. Demirboğa, R. Gül, "The effects of expanded perlite aggregate, silica fume and fly ash on the thermal conductivity of lightweight concrete", Cement and Concrete Research 33(5) (2003) 723-727.

[48] I. Soroka, N. Setter, "The effect of fillers on strength of cement mortars", Cement and Concrete Research 7(4) (1977) 449-456.

[49] V. Yogendran, B.W. Langan, M.N. Haque, M.A. Ward, "SILICA FUME IN HIGH-STRENGTH CONCRETE", ACI Materials Journal 84(2) (1987) 124-129.

[50] J.-Y. Shih, T.-P. Chang, T.-C. Hsiao, "Effect of nanosilica on characterization of Portland cement composite", Materials Science and Engineering: A 424(1) (2006) 266-274.

[51] I. Schachinger, H. Hilbig, T. Stengel, E. Fehling, "Effect of curing temperature at an early age on the long-term strength development of UHPC", 2nd International Symposium on Ultra High Performance Concrete 10 (2008) 205-213.

[52] H.F.W. Taylor, C. Famy, K.L. Scrivener, "Delayed ettringite formation", Cement and Concrete Research 31(5) (2001) 683-693.

[53] S.-H. Kang, J.-H. Lee, S.-G. Hong, J. Moon, "Microstructural Investigation of Heat-Treated Ultra-High Performance Concrete for Optimum Production", Materials (Basel, Switzerland) 10(9) (2017) 1106.

# 국문초록

## 낮은 물-시멘트에서 다량의 세노스피어의 혼입을 통한 고강도 및 경량 시멘트 복합체 개발

조티 마하토

건설환경공학부

서울대학교 공과대학

사회 인프라 및 도시화 수요의 급속한 증가로인해 경량 콘크리트의 수요가 높아지고있다. 하지만 경량 콘크리트에 사용되는 경량 골재는 낮은 밀도로인해 강도발현에 어려움이있다. 또한 낮은 밀도의 경량 콘크리트는 골재분리 현상에 취약한 특성을 지니고있다. 추가로 지구 온난화는 에너지 효율적이고 에너지 절약형 콘크리트 재료의 사용을 요구한다. 따라서 본 연구는 세노스피어를 이용한 압축 강도가 높고 밀도가 낮으며 열전도율이 낮은 경량 시멘트 복합체를 제작하는 것을 목표로한다.

본 논문에서는 세노스피어를 시멘트 대비 10 및 20 wt.%로 첨가했다. 낮은 물- 시멘트 비율을 도입하였으며 상온양생과 고온양생을 진행하였다. 상온양생은 20 °C 의 RH 60% 환경에서 수행되었으며 고온양생의 경우 90 °C 에서 이틀 간 수행되었다. 또한 X-ray 회절 (XRD) 및 열 중량 분석

(TGA)을 수행하여 원재료와 시편의 광물 학적 특성을 얻고 수화물의 상 변화를 정성적으로 분석했다. 세노스피어의 분리와 표본의 내부 미세 구조는 micro-computed tomography 를 사용하여 연구되었다.

그 결과 상온 (20ºC 및 RH 60 %)에서 경화 된 개발 된 시멘트 복합체는 74 ~ 64MPa 의 우수한 압축 강도를 보였으며 고온환경 (HT 90ºC)에서 경화 된 시멘트 복합체는 90 ~ 87MPa 의 압축 강도와 낮은 밀도, 낮은 열전도도를 나타냈다. 또한, 제작 된 배합 설계에서는 골재분리현상이 일어나지않았다. 배합에서의 세노스피어의 균일 한 분산이 마이크로 CT 촬영을 통해 확인되었고 그 현상이 정량화가 계산되었다. 더욱이 공극구조의 결과는 개발 된 복합 재료가 염해 환경 저항성을 지닌 것으로도 해석할 수 있어 염해 환경에 노출 된 구조물에서의 사용 가능성이 크다는 것을 보여준다.

키워드: 경량 복합재; 세노스피어; 열 전도성; XRD 및 TGA; 마이크로 컴퓨터 단층 촬영; 다공성.

학번: 2019-27932